Baird's Diradicals

Deutsche Ausgabe: DOI: 10.1002/ange.201500879
Internationale Ausgabe: DOI: 10.1002/anie.201500879

An Unusually Small Singlet–Triplet Gap in a Quinoidal 1,6-Methano[10]annulene Resulting from Baird's 4*n* π-Electron Triplet Stabilization**

Benjamin C. Streifel, José L. Zafra, Guzmán L. Espejo, Carlos J. Gómez-García, Juan Casado, and John D. Tovar**

Abstract: *Within the continuum of π-extended quinoidal electronic structures exist molecules that by design can support open-shell diradical structures. The prevailing molecular design criteria for such structures involve proaromatic nature that evolves aromaticity in open-shell diradical resonance structures. A new diradical species built upon a quinoidal methano[10]annulene unit is synthesized and spectroscopically evaluated. The requisite intersystem crossing in the open-shell structure is accompanied by structural reorganization from a contorted Möbius aromatic-like shape in S_0 to a more planar shape in the Hückel aromatic-like T_1. This stability was attributed to Baird's Rule which dictates the aromaticity of 4n π-electron triplet excited states.*

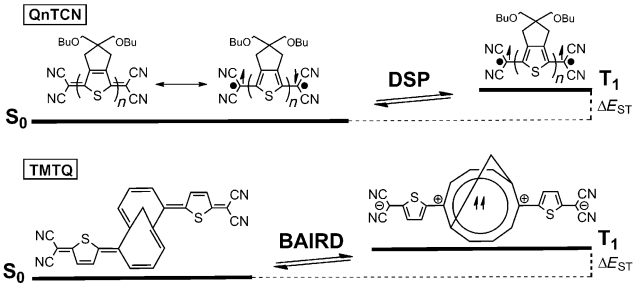

Scheme 1. Quinoidal (closed-shell)–aromatic (open-shell) transformations in the QnTCN family ($n = 1$–6, top, along with the equilibrium with the triplet) and in TMTQ (bottom). DSP: double spin polarization.

π-Conjugated molecules with distinctly quinoidal structures have unique electronic, magnetic, and optical properties that make them well suited for a variety of organic electronic,[1] spintronic,[2] and energy-storage applications.[3] Two common motifs for these molecules are extended polycyclic aromatic frameworks[4–7] and conjugated oligomers with terminal dicyanomethylene groups (e.g. QnTCN, Scheme 1).[8–10] Molecules with extended quinoidal structures often exhibit strong electron-accepting behavior, with electron mobilities well over 1 $cm^2 V^{-1} s^{-1}$.[11,12]

These quinoidal platforms typically have a proaromatic character, which makes them convertible into aromatic moieties, thus opening a dichotomy of closed-shell quinoidal or open-shell diradical structures (Scheme 1). For QnTCN, the smaller oligomers (Q1TCN, Q2TCN, Q3TCN) bear closed-shell full quinoidal structures, while longer analogues (Q5TCN, Q6TCN) are Kekulé diradicals.[9] The latter are characterized by singlet electronic ground states because of double spin polarization (DSP), which preferably stabilizes the singlet over the triplet diradical state and thus controls the singlet–triplet energy gap (ΔE_{ST} in Scheme 1).[13–15] ΔE_{ST} thus becomes the fingerprint of a Kekulé diradical. Molecules in this quinoidal–diradical landscape offer interesting properties, such as magnetic switching, strong NIR two-photon absorption, and singlet–exciton fission.[16]

Several groups are now studying new co-oligomers that assemble distinctive proaromatic units as a way to adjust the ΔE_{ST},[17,18] some of which are ground-state Kekulé diradicals (Scheme 2).[19–21] Q2TCN[22] and 1PerTCN[23] in Schemes 1 and 2 have very high ΔE_{ST} gaps, but perylene insertion between the bithiophene moiety (e.g., Q2-1PerTCN, Scheme 2) leads to an ΔE_{ST} of −4.71 kcal mol^{-1}, and a perylene dimer (2PerTCN) displays an ΔE_{ST} of −4.15 kcal mol^{-1}.[21,23] Ladder-type conjugated oligomers can further reduce the gap to 2.12 kcal mol^{-1}.[7] These additional modulations are obviously in accordance with the degree of aromaticity of the rings created upon the formation of the diradical and by the facility of DSP.

Herein, we focus on a building block that is unprecedented in the chemistry of Kekulé diradicals: Vogel's classic 1,6-methano[10]annulene (M10A) hydrocarbon.[24] M10A can be viewed as on the border between a classical Hückel aromatic and a cyclic polyene because of its nonplanarity and relatively low aromatic stabilization energy,[25] and it is known to stabilize radical species.[26] M10A can also be a useful component of conjugated aromatic polymers and oligomers by lowering oxidation potentials, increasing effective conjugation lengths, and stabilizing reactive comonomers.[27,28] The

[*] Dr. B. C. Streifel, Prof. J. D. Tovar
Department of Chemistry, Johns Hopkins University
Baltimore MD, 21218 (USA)
E-mail: tovar@jhu.edu
Prof. C. J. Gómez-García
Instituto de Ciencia Molecular, Universidad de Valencia
46980 Paterna (Spain)
Dr. J. L. Zafra, G. L. Espejo, Prof. J. Casado
Department of Physical Chemistry, University of Málaga
Campus de Teatinos s/n, 29071 Málaga (Spain)
E-mail: casado@uma.es

[**] Financial support from MINECO (CTQ2012-33733 and CTQ2011-26507), Junta de Andalucía (P09-FQM-4708), GV (Prometeo II/2014/076) and the National Science Foundation (DMR-1207259, J.D.T.) is acknowledged.

Supporting information for this article is available on the WWW under http://dx.doi.org/10.1002/anie.201500879.

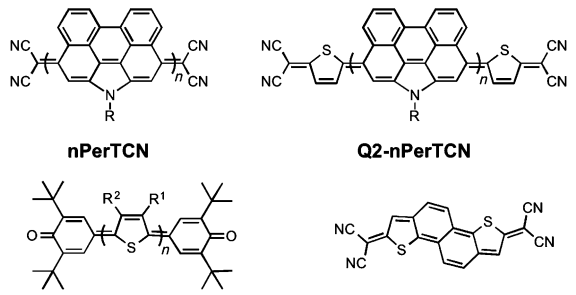

Scheme 2. Examples of thiophene-containing molecules that lie within the quinoidal–diradical continuum in S_0. Clockwise from top left: nPerTCN ($n=1$, 2);[23] Q2-nPerTCN ($n=1$, 2);[21] dithienonaphthalene,[10] and diphenoquinone oligothiophenes ($n=2$, 3, 4).[19,20]

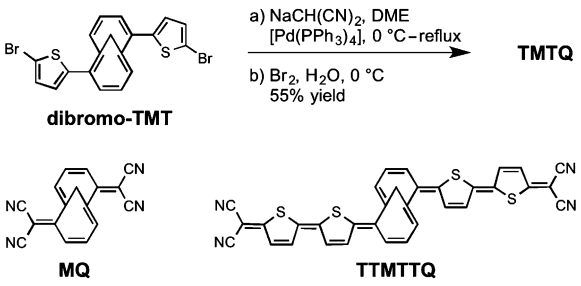

Scheme 3. Synthesis of TMTQ through the Takahashi method. Related compounds MQ and TTMTTQ could not be synthesized by this route.

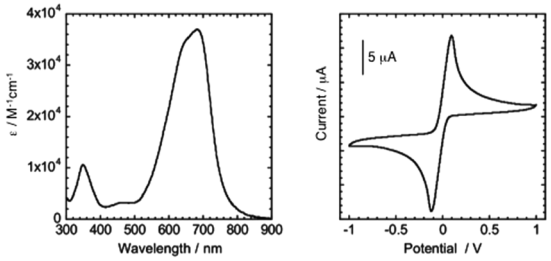

Figure 1. UV-Vis absorption spectrum ($CHCl_3$, left) and cyclic voltammogram (THF/TBAP, right) of TMTQ.

bridging methylene of M10A frustrates π-stacking interactions and results in solution-processable semiconducting polymers.[29] These properties make M10A an attractive target for incorporation into quinoidal motifs with the aim of creating unique Kekulé diradicals with tunable ΔE_{ST}.

We present an M10A co-oligomer in a quinoidal configuration (TMTQ, Scheme 1), wherein the M10A occupies a substantially reduced molecular footprint compared to other proaromatic subunits. We compared the properties of TMTQ with those of known and previously studied QnTCN analogues,[30] and we found evidence for its diradicaloid character at room temperature with a surprisingly low ΔE_{ST} gap of $-4.86\,kcal\,mol^{-1}$. This makes it one of the shortest isolable diradical-supporting π-conjugated molecular structures reported to date. We justify the low ΔE_{ST} gap on the basis of the exclusive aromatic stabilization of the triplet excited state (T_1), as described by Baird's rule (Scheme 1).[31,32] This represents a novelty compared with most of the existing Kekulé diradicals, in which the small ΔE_{ST} gaps result from the particular influence of DSP on their open-shell diradical singlet ground electronic states, wherein more bonding implies larger ΔE_{ST} (their triplet excited state energies are much less affected). However, ΔE_{ST} in TMTQ is the result of the triplet state stabilization resulting from Baird aromaticity recovery.

The synthesis of TMTQ (Scheme 3) was accomplished by Takahashi coupling.[33] The sodium salt of malononitrile was coupled to dibromo-TMT[29] under Pd catalysis and the coupling product was oxidized with Br_2 in water. TMTQ was purified and isolated as a dark blue solid. Attempts to synthesize related molecules MQ and TTMTTQ (Scheme 3) were not successful.

The UV-Vis spectrum of TMTQ shows an absorption peak at 683 nm ($\varepsilon = 37000\,M^{-1}\,cm^{-1}$) with an onset at 850 nm (Figure 1), assigned as the HOMO–LUMO transition with (U)B3LYP/6-31G** TD-DFT calculations (Figure S4 and S14). Intense low-energy absorption features are common among tetracyanoquinodimethanes because of low-lying LUMO levels imparted by the electron-deficient dicyanomethylene units and the high HOMO energies associated with the conjugated bridges. The absorption spectra of TMTQ, Q2TCN, and Q3TCN follow a trend in increasing λ_{max} with increasing conjugation length, with TMTQ falling between Q3TCN ($\lambda_{max} = 646$ nm) and Q4TCN ($\lambda_{max} =$ 780 nm; Figure S5). Photoluminescence studies of TMTQ show a lack of significant emission upon excitation of the main absorption band (Figure S6). Cyclic voltammetry shows a reversible peak at −12 mV vs. Ag/Ag^+ ($E_{1/2}$), corresponding to an electrochemical LUMO of −4.18 eV (calculated as −4.18 eV, Figure S14), indicating the strong electron-accepting, and therefore easily reducible, nature of TMTQ (Figure 1, right). Attempts to oxidize TMTQ electrochemically resulted in irreversible decomposition.

Variable-temperature ^1H NMR experiments (Figure S7–S9) suggest interconversion between quinoidal and diradical states. At 25 °C, there is evidence of some paramagnetic broadening of the signals, indicating the interference of a possible open-shell magnetically active species. As the temperature is raised to 100 °C, there is a loss of resolution and the growth of broad, featureless resonances around 7.26, 6.40, and 5.85 ppm, but the broad nature of the resonances does not allow any structural assignment. Upon cooling to 0 °C, the resolution of the signals is enhanced, suggesting a less paramagnetic character.

TMTQ shows a narrow and weak EPR signal in the solid state and in $CHCl_3$ with $g \approx 2.004$ and a line-width of around 7.5 G at 298 K because of the presence of magnetically active species in both phases (Figure 2 and S10). The intensity of the solid-state EPR signal decreases with the temperature and reaches a rounded minimum at approximately 150 K. A very small fraction of isolated radical paramagnetic impurity (ca. 0.5 % after SQUID measurements, see below) accounts for the EPR signal below 150 K. Magnetic susceptibility measurements (Figure 2) show a decrease of the $\chi_m T$ product (χ_m = molar magnetic susceptibility) from around $0.008\,cm^3\,K\,mol^{-1}$ at 400 K to about $0.002\,cm^3\,K\,mol^{-1}$ at 250 K. Below 250 K, $\chi_m T$ remains constant. This behavior indicates the presence of

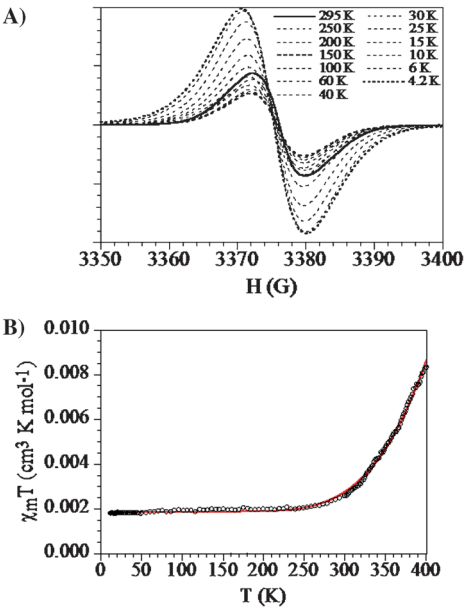

Figure 2. Top: X-band variable-temperature solid-state EPR spectra of TMTQ. Bottom: χ_m *T-T* curve in the SQUID measurements for TMTQ powder. The solid line is the fit to the Bleaney–Bowers equation.

a magnetically active state that is only populated at high temperatures. The χ_m *T-T* fitting to the Bleaney–Bowers equation (solid line in Figure 2) provides an experimental $\Delta E_{ST} = -4.86\ \text{kcal mol}^{-1}$, meaning that in S_0 there is a strong antiferromagnetic coupling or closed-shell character, while heating significantly populates a low-lying T_1. (U)B3LYP/6-31G** DFT calculations predict $\Delta E_{ST} = -4.38\ \text{kcal mol}^{-1}$ in very nice agreement with the experiment. This ΔE_{ST} is remarkably low in comparison with other parent structures of comparable size (Q3TCN: $\Delta E_{ST} = -6.89\ \text{kcal mol}^{-1}$, Q4TCN: $\Delta E_{ST} = -4.06\ \text{kcal mol}^{-1}$, Q21PerTCN: $\Delta E_{ST} = -4.71\ \text{kcal mol}^{-1}$). Other similar compounds, in which the M10A unit is replaced by naphthyl groups, give $\Delta E_{ST} < -10\ \text{kcal mol}^{-1}$, and oligoquinones of similar size (e.g. thienyl heteroquaterphenoquinones)[19] do not show triplet diradical character.

The intrinsically chiral and nonplanar structure of the M10A subunit prevents X-ray crystallographic analysis. Infrared and Raman spectroscopic analyses, in turn, have been used to infer structural details of diradical singlet and triplet species.[23,34] Figure 3 shows the infrared spectra of Q2TCN, Q3TCN, and TMTQ: the $\tilde{\nu}$(C≡N) wavenumber is a good marker of the electron density on the dicyano groups because of their electron-withdrawing nature (Figure S17,18).[35] The lowest wavenumber for TMTQ at 2208 cm^{-1} suggests a greater electron density on the CN groups compared to Q2TCN (2216 cm^{-1}) and Q3TCN (2210 cm^{-1}). This means that the central dithienyl–M10A unit complementarily bears an equivalent amount of positive charge. By heating TMTQ, the $\tilde{\nu}$(C≡N) band decreases by around 4 cm^{-1}, indicating a greater shift of electron density toward the CN groups (through the development of more diradical character, see Figure S11 and Scheme S2).

The Raman spectra of Q3TCN and TMTQ are also shown in Figure 3. In fully quinoidal Q3TCN, the main Raman bands are at 1430 and 1405 cm^{-1}, while the fully aromatic α,α′-dicyano terthiophene (T3CN2, Figure 3) shows this mode at 1456 cm^{-1}.[36,37] This signature falls at 1441 cm^{-1} for TMTQ, suggesting that S_0 of TMTQ lies between the quinoidal Q3TCN and aromatic T3CN2 extremes. The Raman spectrum also presented for Q2-1PerTCN shows the thiophene mode at 1492 cm^{-1}, thus indicating complete thienyl aromatization and a large diradical character imparted by DSP and steric hindrance. Thus, the S_0 of TMQT is charge polarized and intermediate between quinoidal and aromatic (**A** in Scheme 4). Figure S12 compares TMQT with other QnTCNs.

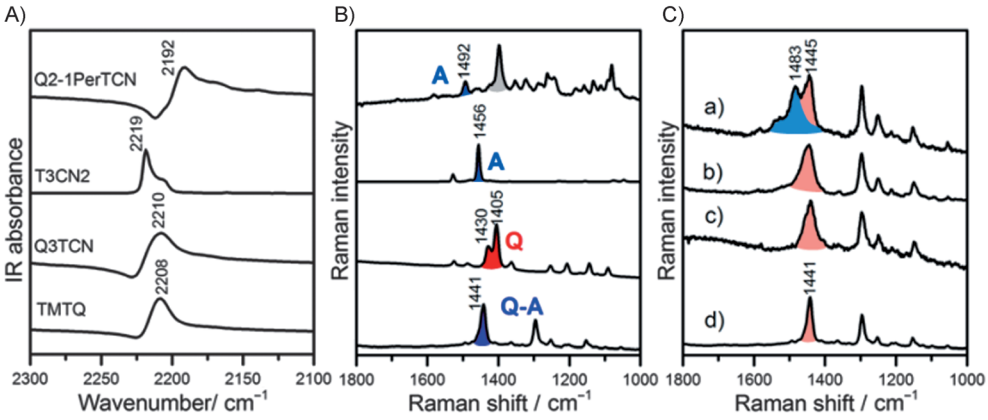

Figure 3. Left: infrared spectra in the $\tilde{\nu}$(CN) region. Middle: Raman spectra (A: full aromatic, Q: full quinoidal, Q-A: intermediate). Right: Raman spectra of TMTQ at different excitation wavelengths: a) 532 nm, b) 633 nm, c) 785 nm, and d) 1064 nm. In solid state at 298 K.

Baird's rule for antiaromatic molecules establishes that the T_1 and S_1 excited states of $4n$ π-electron systems are stabilized by aromaticity.[31] The T_1 stabilization has been probed for a series of antiaromatic molecules that shows rather small ΔE_{ST} gaps, and NICS values for the T_1 states show their aromatization.[32,38] The electron-withdrawing nature of the dicyanomethylene groups leaves a significant portion of positive charge in the TMTQ bridge, particularly in M10A, so the canonical structure **A** in Scheme 4 might have an important contribution to S_0. Structure **A** has eight electrons in conjugation within the central M10A, corresponding to a Hückel antiaromatic structure. Therefore, by considering Baird's rule, the T_1 state of this [10]annulene dication should be largely stabilized (**B** in Scheme 4). In line with our discussion, the [10]annulene dication has been proposed to be stabilized by Möbius aromaticity.[39]

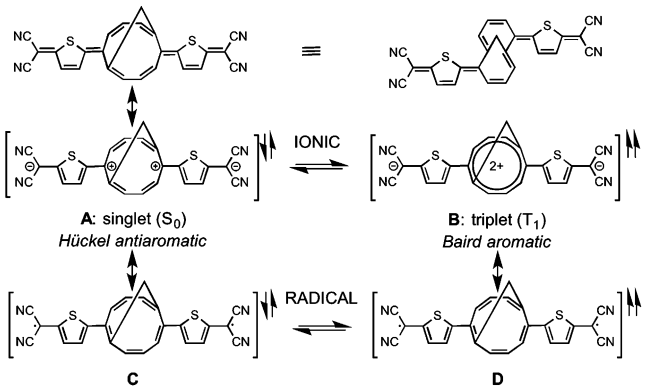

Scheme 4. Closed-shell (top), ionic (**A** and **B**), and diradical (**C** and **D**) canonical forms for S_0 and T_1 of TMTQ. The central M10A ring has been distorted for clarity.

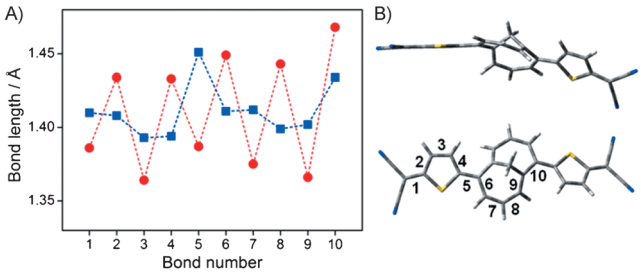

Figure 4. Left: (U)B3LYP/6-31G** DFT calculated bond lengths for S_0 (circles) and T_1 (squares). Right: Frontal and top views of the S_0-optimized structure of TMTQ.

This explanation for the small $\Delta E_{ST} = -4.86$ kcal mol^{-1} is further in agreement with: 1) The ^{1}H NMR spectra, which show an equilibrium between a closed-shell singlet (the charge-polarized ground electronic state) and a thermally accessible triplet; 2) the low-energy $S_0 \rightarrow S_1$ UV-Vis absorption compared to Q2TCN and Q3TCN because of the partial aromatic recovery ("Baird's stabilization") in S_1; 3) the low $\tilde{\nu}$(C≡N) wavenumber resulting from the pseudo-Möbius [10]annulene dication; and 4) quinoidal-aromatic intermediate closed-shell character for the thiophene unit of TMQT in S_0 from the Raman wavenumbers (T3CN full aromatic > TMQT > Q3TCN full quinoidal) consistent with the closed-shell zwitterionic- or ionic-like form **A** in Scheme 4. TMQT displays a significant solvatochromism (> 40 nm, > 0.1 eV) from hexane to DMSO corroborating a partial zwitterion (Figure S13). Q3TCN also displays similar solvatochromism (≈ 35 nm) or equivalent polarization, however, for Q3TCN no antiaromatic fragments can be drawn (Scheme S3).

We optimized the (U)B3LYP/6-31G** energies of the S_0 ground electronic state of TMTQ as a closed-shell structure (quinoidal form plus zwitterionic-like form **A**) and as an open-shell structure (diradical **C**). Full convergence of both energies was obtained, highlighting the closed-shell nature of S_0 (residual diradical character; see the Supporting Information). The S_0 geometry of TMQT in Figure 4 shows a partial rotation of the outer thiophenes relative to M10A in accordance with the single character of the connecting bond (structure **A**). Calculated atomic charge distributions also support the zwitterionic character (Figure S16). The M10A shows a contorted structure, or Möbius-like aromatic shape. (U)B3LYP/6-31G** bond lengths for the C–C skeleton of TMTQ are given in Figure 4. The S_0 state showed bond alternation in agreement with the intermediate quinoidal/aromatic structure. The T_1 conversely shows a low degree of bond length alternation within the rings, confirming the proposed aromatic-like structure stabilized in a Baird sense. Bond 5 in T_1 is very long as a result of steric/torsional strain (structure **A**).[29]

The Raman spectrum with the 532 nm laser excitation in Figure 3 displays a new peak at 1483 cm^{-1} together with that at 1441–1445 cm^{-1} typical of the 1064/785/633 nm laser Raman excitations. Hence, the growth of a new band in the 532 nm Raman spectrum displaced at higher wavenumber, 1445→1482 cm^{-1}, is in line with the up-shift of the Raman bands from the Q3TCN quinoidal to the T3CN aromatic, 1430→1456 cm^{-1}, and suggests a change toward a much more aromatic core such as in the triplet structure **D** in Scheme 4. $T_1 \rightarrow T_n$ absorptions are likely excited with the 532 nm laser, resulting in resonance enhancement of the Raman bands of the TMQT triplet species that becomes visible, despite being present in very small amounts. Although we were unable to detect these absorptions using microsecond flash photolysis (likely because of the anticipated short lifetime of the triplet state), TD-DFT calculations show a strong transition at 570 nm that could be resonantly excited in the Raman experiment at 532 nm excitation (Figure S15). A very similar result happens in the detection of the triplet species of Q6TCN by resonance Raman.[22]

UV-Vis, infrared, and Raman spectroelectrochemical analyses of TMTQ were performed during reduction to the dianion (Figure 5). The 683 nm UV-Vis absorption of the neutral TMTQ progressively disappears along with the growth of a new band at 521 nm. The 683→521 nm blue-shift is a result of the full aromatization of the pseudo-quinoidal S_0 upon reduction, supported by the 1441→1455 cm^{-1} upshift of the Raman band from the neutral species to the dianion (Figure 5c). Reduction also led to the disappearance of the $\tilde{\nu}$(C≡N) band at 2214 cm^{-1} accompanied by the appearance of a new signal at 2168 cm^{-1}. The 2214→2168 cm^{-1} downshift is rationalized by the accumulation of charge in the vicinity of the cyano groups. The direct generation of the dianion is driven by: 1) the inherent electron-withdrawing CN groups; 2) the aromatization process of the pseudo-quinoidal thiophenes; 3) the electron-deficient character of the M10A unit (pseudo [10]annulene dication); and 4) the propensity to recover aromaticity of the $4n$ π-electron M10A structure from 8 ($4n$, $n = 2$, **A** in Scheme 4) to 10 electrons ($4n + 2$, $n = 2$).

In conclusion, to the best of our knowledge, TMTQ is one of the unique cases in which the diradical property in carbon-based metal-free conjugated cores is expressed because of a small ΔE_{ST} gap imparted by the net stabilization of its first triplet excited state. This is due to the recovery of aromaticity from an antiaromatic fragment in the excited state as dictated by Baird's rule for $4n$ π-electron systems. This is a distinctive and unique feature compared with parent carbon-based

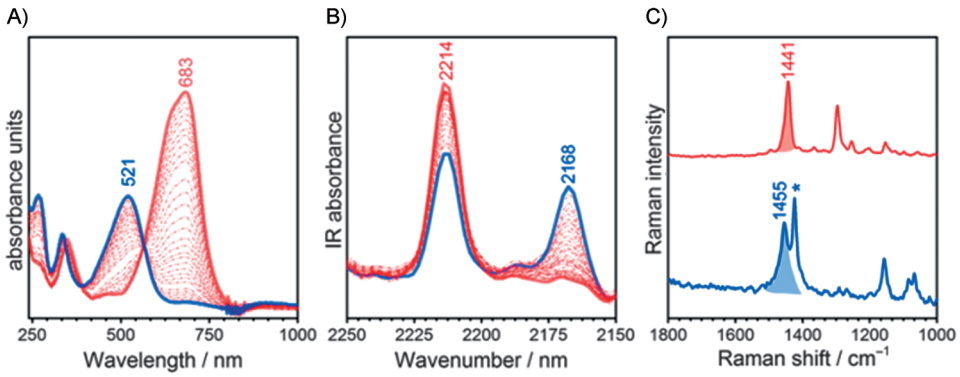

Figure 5. UV-Vis (left) and infrared absorption (center) spectra recorded during the electrochemical reduction of TMTQ. FT-Raman spectra (right) of neutral and reduced species of TMTQ. Red line: neutral, blue line: after reduction.

Kekulé diradicals, which display the same magnitude of ΔE_{ST} gaps conversely resulting from the extensive aperture of the closed-shell ground electronic structure. Although the singlet–triplet gap in Kekulé diradicals involves a pure electronic effect (DSP), the $S_0 \rightarrow T_1$ intersystem crossing in TMTQ can be accompanied by structural reorganization from a contorted Möbius aromatic-like shape in the [10]annulene dication fragment in S_0 to a more planar shape in the Hückel aromatic-like T_1. This stable thiophene/[10]annulene co-oligomer represents a new example of modulation of the ΔE_{ST} gap by specific chemical design by combining non-aromatic (proaromatic) and antiaromatic cores and therefore holds a promising future in the physical organic chemistry of π-conjugated spin-bearing materials.

Keywords: annulenes · aromaticity · Baird's rule · diradical species · quinoidal structures

How to cite: *Angew. Chem. Int. Ed.* **2015**, *54*, 5888–5893
Angew. Chem. **2015**, *127*, 5986–5991

[1] T. M. Pappenfus, R. J. Chesterfield, C. D. Frisbie, K. R. Mann, J. Casado, J. D. Raff, L. L. Miller, *J. Am. Chem. Soc.* **2002**, *124*, 4184–4185.
[2] Y.-W. Son, M. L. Cohen, S. G. Louie, *Phys. Rev. Lett.* **2006**, *97*, 216803.
[3] Y. Morita, S. Nishida, T. Murata, M. Moriguchi, A. Ueda, M. Satoh, K. Arifuku, K. Sato, T. Takui, *Nat. Mater.* **2011**, *10*, 947–951.
[4] A. Konishi, Y. Hirao, M. Nakano, A. Shimizu, E. Botek, B. Champagne, D. Shiomi, K. Sato, T. Takui, K. Matsumoto, H. Kurata, T. Kubo, *J. Am. Chem. Soc.* **2010**, *132*, 11021–11023.
[5] A. Shimizu, R. Kishi, M. Nakano, D. Shiomi, K. Sato, T. Takui, I. Hisaki, M. Miyata, Y. Tobe, *Angew. Chem. Int. Ed.* **2013**, *52*, 6076–6079; *Angew. Chem.* **2013**, *125*, 6192–6195.
[6] G. E. Rudebusch, A. G. Fix, H. A. Henthorn, C. L. Vonnegut, L. N. Zakharov, M. M. Haley, *Chem. Sci.* **2014**, *5*, 3627–3633.
[7] X. Zhu, H. Tsuji, K. Nakabayashi, S.-i. Ohkoshi, E. Nakamura, *J. Am. Chem. Soc.* **2011**, *133*, 16342–16345.
[8] T. Takahashi, K. I. Matsuoka, K. Takimiya, T. Otsubo, Y. Aso, *J. Am. Chem. Soc.* **2005**, *127*, 8928–8929.
[9] J. Casado, R. Ponce Ortiz, J. T. López Navarrete, *Chem. Soc. Rev.* **2012**, *41*, 5672–5686.
[10] T. Mori, N. Yanai, I. Osaka, K. Takimiya, *Org. Lett.* **2014**, *16*, 1334–1337.
[11] R. J. Chesterfield, C. R. Newman, T. M. Pappenfus, P. C. Ewbank, M. H. Haukaas, K. R. Mann, L. L. Miller, C. D. Frisbie, *Adv. Mater.* **2003**, *15*, 1278–1282.
[12] C. Zhang, Y. Zang, E. Gann, C. R. McNeill, X. Zhu, C.-a. Di, D. Zhu, *J. Am. Chem. Soc.* **2014**, *136*, 16176–16184.
[13] W. T. Borden in *Diradicals* (Ed.: W. T. Borden), Wiley Interscience, New York, **1982**, pp. 3–65.
[14] P. Karafiloglou, *J. Chem. Educ.* **1989**, *66*, 816–818.
[15] W. T. Borden, H. Iwamura, J. A. Berson, *Acc. Chem. Res.* **1994**, *27*, 109–116.
[16] Z. Sun, Z. Zeng, J. Wu, *Acc. Chem. Res.* **2014**, *47*, 2582–2591.
[17] T. M. Pappenfus, B. J. Hermanson, T. J. Helland, G. G. W. Lee, S. M. Drew, K. R. Mann, K. A. McGee, S. C. Rasmussen, *Org. Lett.* **2008**, *10*, 1553–1556.
[18] J. Casado, M. Z. Zgierski, P. C. Ewbank, M. W. Burand, D. E. Janzen, K. R. Mann, T. M. Pappenfus, A. Berlin, E. Pérez-Inestrosa, R. Ponce Ortiz, J. T. López Navarrete, *J. Am. Chem. Soc.* **2006**, *128*, 10134–10144.
[19] E. V. Canesi, D. Fazzi, L. Colella, C. Bertarelli, C. Castiglioni, *J. Am. Chem. Soc.* **2012**, *134*, 19070–19083.
[20] K. Takahashi, T. Suzuki, *J. Am. Chem. Soc.* **1989**, *111*, 5483–5485.
[21] Z. Zeng, S. Lee, J. L. Zafra, M. Ishida, N. Bao, R. D. Webster, J. T. López Navarrete, J. Ding, J. Casado, D. Kim, J. Wu, *Chem. Sci.* **2014**, *5*, 3072–3080.
[22] R. Ponce Ortiz, J. Casado, V. Hernández, J. T. López Navarrete, P. M. Viruela, E. Orti, K. Takimiya, T. Otsubo, *Angew. Chem. Int. Ed.* **2007**, *46*, 9057–9061; *Angew. Chem.* **2007**, *119*, 9215–9219.
[23] Z. Zeng, M. Ishida, J. L. Zafra, X. Zhu, Y. M. Sung, N. Bao, R. D. Webster, B. S. Lee, R.-W. Li, W. Zeng, Y. Li, C. Chi, J. T. López Navarrete, J. Ding, J. Casado, D. Kim, J. Wu, *J. Am. Chem. Soc.* **2013**, *135*, 6363–6371.
[24] E. Vogel, H. D. Roth, *Angew. Chem. Int. Ed. Engl.* **1964**, *3*, 228–229; *Angew. Chem.* **1964**, *76*, 145–145.
[25] W. R. Roth, M. Böhm, H. W. Lennartz, E. Vogel, *Angew. Chem. Int. Ed. Engl.* **1983**, *22*, 1007–1008; *Angew. Chem.* **1983**, *95*, 1011–1012.
[26] X. Creary, K. M. Miller, *Org. Lett.* **2002**, *4*, 3493–3496.
[27] P. A. Peart, J. D. Tovar, *Org. Lett.* **2007**, *9*, 3041–3044.
[28] P. A. Peart, J. D. Tovar, *Macromolecules* **2009**, *42*, 4449–4455.
[29] B. C. Streifel, P. A. Peart, J. F. Martinez Hardigree, H. E. Katz, J. D. Tovar, *Macromolecules* **2012**, *45*, 7339–7349.
[30] R. Ponce Ortiz, J. Casado, V. Hernández, J. T. López Navarrete, E. Orti, P. M. Viruela, B. Milian, S. Hotta, G. Zotti, S. Zecchin, B. Vercelli, *Adv. Funct. Mater.* **2006**, *16*, 531–536.
[31] N. C. Baird, *J. Am. Chem. Soc.* **1972**, *94*, 4941–4948.
[32] M. Rosenberg, C. Dahlstrand, K. Kilsa, H. Ottosson, *Chem. Rev.* **2014**, *114*, 5379–5425.
[33] M. Uno, K. Seto, S. Takahashi, *J. Chem. Soc. Chem. Commun.* **1984**, 932–933.
[34] J. Casado, S. Patchkovskii, M. Z. Zgierski, L. Hermosilla, C. Sieiro, M. M. Oliva, J. T. López Navarrete, *Angew. Chem. Int. Ed.* **2008**, *47*, 1443–1446; *Angew. Chem.* **2008**, *120*, 1465–1468.
[35] J. S. Chappell, A. N. Bloch, W. A. Bryden, M. Maxfield, T. O. Poehler, D. O. Cowan, *J. Am. Chem. Soc.* **1981**, *103*, 2442–2443.

[36] V. Hernández, S. Hotta, J. T. López Navarrete, *J. Chem. Phys.* **1998**, *109*, 2543 – 2548.
[37] J. Casado, R. Ponce Ortiz, M. C. Ruiz Delgado, R. Azumi, R. T. Oakley, V. Hernández, J. T. López Navarrete, *J. Phys. Chem. B* **2005**, *109*, 10115 – 10125.
[38] K. Jorner, R. Emanuelsson, C. Dahlstrand, H. Tong, A. V. Denisova, H. Ottosson, *Chem. Eur. J.* **2014**, *20*, 9295 – 9303.
[39] E.-K. Mucke, B. Schönborn, F. Köhler, R. Herges, *J. Org. Chem.* **2011**, *76*, 35 – 41.

Received: January 29, 2015
Published online: April 1, 2015

